Galactosylated manganese ferrite nanoparticles for targeted MR imaging of asialoglycoprotein receptor

2013 Nanotechnology 24 475103

(http://iopscience.iop.org/0957-4484/24/47/475103)

Nanotechnology **24** (2013) 475103 (9pp) doi:10.1088/0957-4484/24/47/475103

Galactosylated manganese ferrite nanoparticles for targeted MR imaging of asialoglycoprotein receptor

Seung-Hyun Yang[1,2,8], Dan Heo[1,2,8], Eugene Lee[1], Eunjung Kim[3], Eun-Kyung Lim[4], Young Han Lee[1,2,4,5,6], Seungjoo Haam[2,3], Jin-Suck Suh[1,2,4,5,6], Yong-Min Huh[1,2,4,5,6], Jaemoon Yang[1,4] and Sahng Wook Park[6,7]

[1] Department of Radiology, College of Medicine, Yonsei University, Seoul 120-749, Republic of Korea
[2] Nanomedical National Core Research Center, Yonsei University, Seoul 120-749, Republic of Korea
[3] Department of Chemical and Biomolecular Engineering, Yonsei University, Seoul 120-749, Republic of Korea
[4] YUHS-KRIBB Medical Convergence Research Center, Yonsei University, Seoul 120-749, Republic of Korea
[5] Severance Biomedical Science Institute (SBSI), Seoul 120-752, Republic of Korea
[6] Brain Korea 21 plus Project for Medical Science, Yonsei University, Republic of Korea
[7] Department of Biochemistry and Molecular Biology, Institute of Genetic Science, Integrated Genomic Research Center for Metabolic Regulation, College of Medicine, Yonsei University, Seoul 120-752, Republic of Korea

E-mail: swpark64@yuhs.ac

Received 1 June 2013, in final form 17 September 2013
Published 5 November 2013
Online at stacks.iop.org/Nano/24/475103

Abstract
Cancer cells can express specific biomarkers, such as cell membrane proteins and signaling factors. Thus, finding biomarkers and delivering diagnostic agents are important in the diagnosis of cancer. In this study, we investigated a biomarker imaging agent for the diagnosis of hepatic cancers. The asialoglycoprotein receptor (ASGPr) was selected as a biomarker for hepatoma cells and the ASGPr-targetable imaging agent bearing a galactosyl group was prepared using manganese ferrite nanoparticles (MFNP) and galactosylgluconic acid. The utility of the ASGPr-targetable imaging agent, galactosylated MFNP (G-MFNP) was assessed by several methods in ASGPr-expressing HepG2 cells as target cells and ASGPr-deficient MCF7 cells. Physical and chemical properties of G-MFNP were examined using Fourier-transform infrared spectroscopy, dynamic light scattering, zeta potential analysis, and transmission electron microscopy. No significant cytotoxicity was observed in either cell line. Targeting ability was assessed using flow cytometry, magnetic resonance imaging, inductively coupled plasma atomic emission spectroscopy, absorbance analysis, dark-field microscopy, Prussian blue staining, and transmission electron microscopy. We demonstrated that G-MFNP target successfully and bind to ASGPr-expressing HepG2 cells specifically. We suggest that these results will be useful in strategies for cancer diagnoses based on magnetic resonance imaging.

(Some figures may appear in colour only in the online journal)

Abbreviations

ASGPr : asialoglycoprotein receptor;
MFNP : manganese ferrite nanoparticle;
MR : magnetic resonance;
HCC : hepatocellular carcinoma;
P80 : polysorbate 80;
CDI :1,1′-carbonyldiimidazole;
EDA : ethylenediamine;

[8] These authors contributed equally to this work.

EDC : *N*-(3-dimethylaminopropyl)-*N*-ethylcarbodiimide hydrochloride;
sulfo-NHS : *N*-hydroxysulfosuccinimide;
DMEM : Dulbecco's modified Eagle's medium;
PBS : phosphate-buffered saline;
FT-IR : Fourier-transform infrared spectroscopy;
TEM : transmission electron microscopy.

1. Introduction

Molecular imaging technologies using magnetic resonance (MR) imaging have attracted attention and been used widely in the diagnosis and assessment of cancer because it is possible to visualize anatomical detail with high spatial resolution noninvasively [1–3]. In particular, MRI contrast agents are important for molecular imaging technologies using MRI because of their property of enhancing the MR signal. For this reason, manganese ferrite nanoparticles (MFNP) are compatible materials for molecular imaging due to powerful magnetization caused by the presence of the manganese ion [4]. In other words, MFNP can be used as ultra-sensitive MR imaging contrast agents for the diagnosis of cancer. In particular, MFNP-surface modification such as conjugation with targeting moieties, antibodies or peptides [5, 6] facilitates specific delivery of MFNP to molecular markers of cancer cells and more detailed information on molecular targets via MR imaging

The asialoglycoprotein receptor (ASGPr) is a membrane-bound Ca^{2+}-dependent (C-type) lectin, a carbohydrate-binding protein, found abundantly on the surface of parenchymal hepatic cells ($\sim 5 \times 10^5$ ASGPr molecules/cell) [7, 8]. The number of ASGPr reflects the degree of various liver diseases, such as acute hepatitis, chronic hepatitis, autoimmune hepatitis, and cirrhosis [9–11]. Recently, it has been reported that the ASGPr is involved in cancer metastasis by activation of the epidermal growth factor receptor/extracellular-regulated kinase pathway [12]. The receptor interacts with galactose or *N*-acetyl-galactosamine residues at the non-reducing ends of carbohydrates on glycoproteins via a multivalent interaction, which subsequently triggers receptor-mediated endocytotic uptake of the glycoprotein into hepatocytes and hepatocellular carcinoma (HCC) cells [13–16].

For these reasons, the ASGPr is considered as an attractive molecular target for drug development. The utilization of natural molecules containing galactosylated or lactosylated residues such as asialofetuin [17], or synthetic compounds such as glycolipids [18], glycoproteins [19], and galactosylated polymers [20] as drug targeting carriers has resulted in a significant improvement in targeting efficacy to the liver. Furthermore, the imaging of liver with utilization of the ASGPr can provide diagnostic information relevant to liver cancers [21]. In recent studies, hyperbranched poly(amidoamine) nanoparticles [22], albumin nanoparticles [23], quantum dots [24], dendrimers [25], and iron oxide particles [26] with galactosylated residues have been investigated in liver target imaging. Its abundance makes the ASGPr a valuable target for the development of high-affinity ligands for specific delivery of drugs [27], siRNA [28], DNA [29], and imaging agents [22].

In this study, we prepared a biomarker-specific imaging probe based on modified magnetic nanoparticles for MR imaging (figure 1). Highly crystalline MFNP as a *T*2 MR imaging contrast agent were synthesized and enveloped in an aminated amphiphilic surfactant using a nanoemulsion method. Subsequently, the amine groups of water-soluble MFNP (amine-MFNP) were conjugated with carboxyl groups of galactosylgluconic acid to introduce galactosyl groups on the surface of the MFNP. Surface properties, such as the colloidal size, zeta potential and chemical structure, of the galactosylated MFNP (G-MFNP) were investigated in ASGPr-expressing hepatoma cells. The targeting potential of G-MFNP toward ASGPr-expressing cells was examined using dark-field microscopy and Prussian blue staining. In addition, we confirmed endocytosis of G-MFNP by means of a transmission electron microscope (TEM). Quantification of attached G-MFNP toward the ASGPr was by absorbance spectra analysis and conducted using inductively coupled plasma atomic emission spectroscopy. Finally, the abilities of G-MFNP for targeted MR imaging of ASGPr were investigated by *in vitro* MR imaging. In conclusion, we demonstrated that G-MFNP can successfully attach to ASGPr-expressing HepG2 cells, and these results suggest that G-MFNP targeting the ASGPr is useful in the diagnoses and treatment of many liver diseases, such as liver cancer, chronic hepatitis and cirrhosis, guided by MR imaging.

2. Materials and methods

2.1. Materials

Polysorbate 80 (P80), ethylenediamine, 1,1′-carbonyldiimidazole (CDI), 1,4-dioxane (99.8%), and ethylenediamine (EDA) were purchased from Sigma Aldrich Chemical Co. (USA). *N*-(3-dimethylaminopropyl)-*N*-ethylcarbodiimide hydrochloride (EDC) and *N*-hydroxysulfosuccinimide (sulfo-NHS) were purchased from Pierce (USA). Phosphate-buffered saline (PBS; 10 mM, pH 7.4), Dulbecco's modified Eagle's medium (DMEM), fetal bovine serum, and antibiotic–antimycotic solution were purchased from Life Technologies (USA, Gibco brand) and dialysis membrane (molecular weight cut off: 1, 3.5 kDa) was from Spectrum Laboratories (USA). HepG2 and MCF7 cell lines were purchased from American Tissue Type Culture (USA). Ultrapure deionized water was used for all syntheses. All other chemicals and reagents were of analytical grade.

2.2. Synthesis of MFNP

To synthesize monodispersed MFNP, 2 mmol iron (III) acetylacetonate, 1 mmol manganese (II) acetylacetonate, 10 mmol 1,2-hexadecanediol, 6 mmol dodecanoic acid, and 6 mmol dodecylamine were dissolved in 20 ml benzyl ether under an ambient nitrogen atmosphere. The mixture was

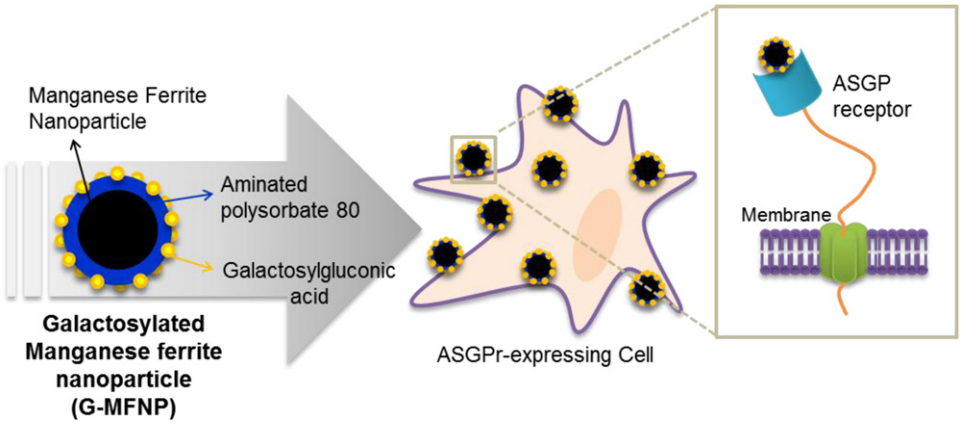

Figure 1. Schematic illustration of the structure of G-MFNP (galactosylated MFNP) for targeted MRI of ASGPr-expressing cells.

pre-heated to 200 °C for 2 h and refluxed at 300 °C for 30 min. After the reactants cooled to room temperature, pure ethanol was added to the mixture and black materials were precipitated and separated by centrifugation (1811 g-force, 10 min). The black precipitates were dissolved in 2 ml hexane in the presence of 80 μmol dodecanoic acid. Centrifugation (1811 g-force, 10 min) was applied to remove any undispersed residues. The 6 nm seeds of MFNP were then precipitated with pure ethanol, centrifuged (1811 g-force, 10 min) to remove the solvent and redispersed into hexane. MFNP approximately 12 nm in diameter were synthesized using the seed-mediated growth method [5, 6].

2.3. Synthesis of aminated P80

To synthesize aminated P80 using CDI as a zero-length cross-linker, 5 mmol P80 and 15 mmol CDI were dissolved in a flask containing 100 ml 1,4-dioxane, and the reaction mixture was stirred for 1 h [30] at room temperature. Subsequently, 15 mmol ethylenediamine was added into the reactor at room temperature. After further reaction for 24 h, unwanted solvent was eliminated using a rotary evaporator. The transparent gel-type remnant was dissolved in 10 ml deionized water and dialyzed against several changes of the excess deionized water for at least seven days. The purified product was freeze dried and stored under vacuum for later use at −70 °C. Synthesis of aminated P80 was confirmed by analyzing its characteristic band using Fourier-transform infrared spectroscopy (FT-IR, Varian, Excalibur series).

2.4. Preparation of amine-MFNP

Water-soluble amine-MFNP were prepared by the nanoemulsion method [5]. In detail, 10 mg MFNP were dissolved in 4 ml hexane (as the organic phase) and the organic phase was mixed with 20 ml deionized water (as the aqueous phase) containing 100 mg aminated P80. After mutual saturation of the organic phase with the aqueous phase, the emulsion was ultra-sonicated in an ice-cooled bath for 15 min at 190 W. The organic solvent was evaporated overnight at room temperature and the products were purified using a centrifugal filter (Centriprep YM-3, 3000 Da MWCO, Amicon, USA) with two cycles at 3000 rpm for 1 h. The size distribution and zeta potential of amine-MFNP were analyzed using laser scattering (ELS-Z, Otsuka Electronics, Japan), with all DLS analysis conducted at pH 5.6. The morphology of amine-MFNP was confirmed using high-resolution transmission electron microscopy (JEM-2100 LAB6, JEOL Ltd Japan).

2.5. Preparation of G-MFNP

For fabrication of the ASGPr-specific nanoprobe, galactosylgluconic acid as a targeting moiety was conjugated on the surface of amine-MFNP using a zero-length cross-linking process [31]. Briefly, 0.76 mmol galactosylgluconic acid was dissolved in 2 ml PBS and mixed with 2 ml amine-MFNP solution (0.85 mg ml^{-1}). Sulfo-NHS (0.3 mmol) and EDC (0.3 mmol) were added to the previous solution. After incubation of the mixture for 24 h at room temperature, the products were purified using a centrifugal filter (3 kDa MWCO) with two cycles at 1811 g for 15 min.

2.6. Cytotoxicity

The cytotoxicities of G-MFNP for HepG2 and MCF7 cells were evaluated using a MTT cell proliferation assay kit I (Roche, SWISS). HepG2 or MCF7 cells were seeded into a 96-well plate at a density of 2×10^4 cells/well and cultured at 37 °C in a humidified atmosphere with 5% CO_2. 24 h after incubation, cells were treated with G-MFNP at various concentrations for 24 h. After treatment, cells were washed with 100 μl PBS, and changed to 100 μl of fresh DMEM. Subsequently, the cells were treated with the MTT assay solution, according to the manufacturer's instructions. Cell viability was evaluated spectrophotometrically using a microplate reader (Synergy H4 hybrid reader, BioTek) at 575 nm (reference wavelength at 650 nm). All experiments were performed in triplicate. Cell viability was determined from the ratio of absorbance values for treated cells to those for non-treated control cells.

2.7. In vitro cell affinity test of G-MFNP

To evaluate the binding affinity of galactosylgluconic acid on ASGPr-expressing cells, the cellular uptake efficacy was confirmed using fluorescence dye conjugated galactosylgluconic acid. This fluorescence particle is prepared by conjugation between galactosylgluconic acid and fluorescein amine using EDC and sulfo-NHS cross-linking method. After suspending HepG2 and MCF7 in 1 mM galactosyl-fluorescein amine solution, cells were incubated in the medium for 30 min at room temperature in the dark. Non-treated cells, the negative control, were deemed 100%. Fluorescence-labeled cells were analyzed by flow cytometry (FACS Calibur, CA, USA).

For the assessment of G-MFNP amount, the absorbance of HepG2 and MCF7 cells treated with G-MFNP was evaluated spectrophotometrically using a microplate reader (Synergy H4 hybrid reader, BioTek). Cells were seeded into a 96-well plate at a density of 2×10^4 cells/well and incubated at 37 °C in a humidified atmosphere with 5% CO_2 After a 24-h incubation, cells were treated with G-MFNP (8 μg ml^{-1}) at 37 °C. The cells were washed with 100 μl PBS. The absorbance of HepG2 and MCF7 cells treated with G-MFNP was evaluated using a microplate reader at 410 nm.

2.8. Dark-field microscopy

HepG2 and MCF7 cells (2.0×10^5 cells/well) were seeded in 24-well plates containing a cover glass and incubated at 37 °C for 24 h. After the incubation with 500 μl of G-MFNP (255 ng ml^{-1}) for 8 h at 37 °C, the cells were washed with PBS and fixed with 4% paraformaldehyde. To determine the binding affinity of the G-MFNP to cells, light scattering images were recorded using an inverted microscope (Olympus BX51, Japan) with a high numerical aperture dark-field condenser (U-DCW, Olympus). Dark-field pictures were captured using an Olympus charge-coupled device camera.

2.9. Prussian blue staining

To evaluate the effect of the cell density on the binding of G-MFNP, HepG2 cells (1.0×10^6 cells/well) were seeded in 6-well plates and incubated for various culture durations at 37 °C, and G-MFNP were treated. After the incubation for 8 h at 37 °C, the cells were washed with PBS and fixed with 4% paraformaldehyde. Potassium ferrocyanide (10%) was mixed 1:1 with 20% HCl. Cells were treated with the mixed solution and incubated for 30 min at RT, and stained with nuclear fast red (Sigma, USA) for 30 min. The cells were observed using an optical microscope (Olympus BX51, Japan).

2.10. Intracellular TEM images

For cellular TEM sample preparation, HepG2 cells (10^6 cells/well) were incubated with G-MFNP (255 ng ml^{-1}) for 30 min on ice and incubated for 30 min at 37 °C. After incubation, cells were washed three times with blocking buffer (0.03% bovine serum albumin, 0.01% NaN_3 in PBS), and fixed for resin-section TEM according to the standard fixation and embedding protocol [5]. Sections were cut using a Leica Ultracut UCT ultra-microtome (Leica Microsystems, Austria). Samples were observed using a transmission electron microscope (TEM, JEM-2100 LAB6, JEOL Ltd Japan).

2.11. In vitro MR imaging of ASGPr

To evaluate the targeted MR imaging of ASGPr and the detection capacity of the G-MFNP, HepG2 and MCF7 cells (10^7 cells/tube) were incubated with G-MFNP (2.55 μg ml^{-1}) for 4 h at 37 °C. After washing away unbound G-MFNP, the $T2$-weighted MR signal intensity of the collected cells was investigated using a 1.5 T clinical MRI instrument (Philips Medical Systems, Best, The Netherlands) with a micro-47 surface coil (Intera; Philips Medical Systems). $R2$ was defined as the inverse of $T2$ relaxation time ($1/T2$, unit: s^{-1}). For $T2$-weighted MR imaging, the following parameters were adopted: resolution of 0.234 mm × 0.234 mm, section thickness of 0.6 mm, TE = 15 ms, TR = 400 ms, and number of acquisitions = 1. After MR imaging, the cellular uptake efficiencies of G-MFNP were quantified via measurement of the magnetic ion (Mn and Fe) concentrations of the MR imaging samples using inductively coupled plasma atomic emission spectroscopy (Thermoelectron Corp.). The untreated cells were used as a negative control.

3. Results and discussion

For targeted MR imaging of ASGPr-expressing cancer cells, first, we need highly magnetic sensitive materials. Iron oxide nanoparticles can be used as excellent MR imaging probes for noninvasive *in vivo* monitoring of molecular and cellular events [32], but we choose MFNP in order to get a greater magnetic susceptibility. MFNP have been previously reported that show a strong MR contrast effect, more than approximately 160% that of iron oxide nanoparticles [4]. MFNP were synthesized by thermal decomposition methods; the size of synthesized MFNP exhibited uniformity, 12 nm in diameter as previously reported [5, 6]. Synthesized MFNP were dispersed in hexane and capped by a fatty acid, dodecanoic acid. To get the water solubility of fatty acid-capped MFNP and to allow conjugation with the targeting moiety (galactosylgluconic acid), the hydroxyl group of P80 was modified with amine groups using EDA and CDI as a zero-length cross-linker. The hydroxyl group of P80 was activated with CDI and the conjugated imidazole group of activated P80 was attacked by the amine group of EDA. Subsequently, a stable carbamate bond was formed by coupling of the hydroxyl group of P80 with the amine group of EDA. Amine-MFNP were prepared by coating with aminated P80 using a nanoemulsion method [5]. As the final product, G-MFNP were synthesized using EDC and sulfo-NHS, cross-linker of amine–carboxyl group, amine groups of amine-MFNP were conjugated with the carboxyl group of galactosylgluconic acid.

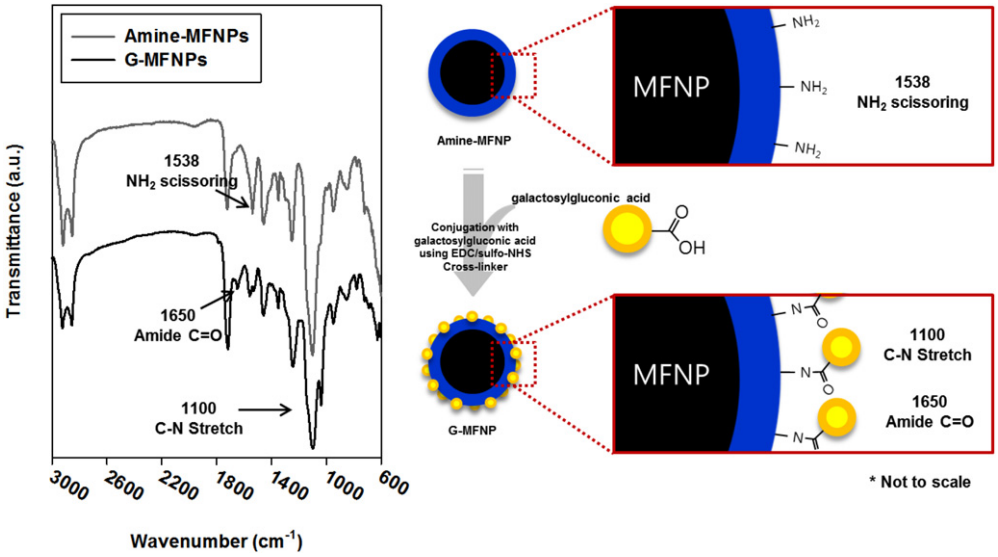

Figure 2. FT-IR spectra of amine-MFNP (upper gray line), G-MFNP (lower black line) and the schematic illustration for the chemical structure of G-MFNP.

After synthesis of G-MFNP, we carried out physico-chemical analysis to investigate the abilities of targeting ASGPr-expressing cancer cells and as a MR contrast agent. First, to investigate chemical conjugation of the amide bond of G-MFNP caused by cross-linking between the amine group (amine-MFNP) and the carboxyl group (galactosylgluconic acid), the characteristic bands of G-MFNP were confirmed using FT-IR. The FT-IR spectrum of amine-MFNP exhibited amine scissoring at 1538 cm^{-1} and the C=O stretch due to amide bonding was observed at 1650 cm^{-1} after conjugation of galactosylgluconic acid (figure 2, arrow). Next, colloidal stabilities were determined by dynamic light scattering. Although the galactosylgluconic acid was conjugated on amine-MFNP, the colloidal diameters of amine-MFNP (30.6 $\pm$ 7.4 nm) and G-MFNP (30.7 $\pm$ 7.6 nm) were similar because of the small molecular size of galactosylgluconic acid (approximately 1.2 nm simulated by ChemSketch Freeware, ACD/Labs, USA). In contrast, the conjugation of galactosylgluconic acid to MFNP changed the surface charge of G-MFNP markedly from 23.2 $\pm$ 1.9 mV (amine-MFNP) to 0.5 $\pm$ 1.3 mV (figure 3(b)). The neutralization of the surface charge reflects that the conjugation of galactosylgluconic acid on the surface of amine-MFNP was successful for ASGPr-specific targeting. Moreover, G-MFNP were enveloped by galactosyl P80, which gives great colloidal stability due to the steric hindrance effect from polyethyleneglycol chains. Thus, the steric hindrance effect of galactosyl P80 plays an important role in the colloidal stability of G-MFNP without any aggregation [33]. As described in the schematic illustration of figure 1, aminated P80 exist on the surface of MFNP, galactosylgluconic acid may exist on the surface of G-MFNP because galactosylgluconic acid is bound together with the terminal amine group of aminated P80 with an amide bond. In transmission electron microscopy, the image of amine-MFNP and G-MFNP showed no significant difference in size or morphology (figure 3(c)). In figure 3, G-MFNP maintains the monodispersed state, not aggregation or changing morphology after surface modification. These results demonstrate that G-MFNP were stably synthesized as designed.

To evaluate ASGPr-specific MR imaging potential of G-MFNP, HepG2 and MCF7 cells were used and thus the binding affinity of galactosylgluconic acid to ASGPr-expressing cell was confirmed on HepG2 and MCF7 cells by flow cytometry. We prepared galactosyl fluorescein as a fluorescence label by the conjugation of fluorescein amine to galactosylgluconic acid. In fluorescence-activated cell sorting analyses, HepG2 cells showed the higher $\Delta FI/FI_{control}$ (FI: fluorescence intensity, control: untreated cells) ratio by a factor of 3.4 times that of MCF7 (control) cells (figure 4(a)). These results support HepG2 cells being suitable for the evaluation of targeting of G-MFNP, and that MCF7 cells can be used as a negative control due to their lack of ASGPr [25, 34–36]. Cytotoxicity of G-MFNP to HepG2 and MCF7 cells was assessed using the MTT assay in eight concentrations; highest concentration: 0.41 μg ml^{-1}, it is diluted tenfold respectively, made seven aliquots (figure 4(b)). Neither HepG2 nor MCF7 cells were damaged significantly by treatment with G-MFNP at the range of concentration used in this study. This is meaningful result when it is interpreted with the results of zeta potential analysis and FT-IR spectra. As previously mentioned, G-MFNP exhibited neutral zeta potential and the amide bond formed by conjugation between the carboxyl groups of galactosylgluconic acid and aminated MFNP. These results reflect that galactosylgluconic acid was well conjugated on the surface of the G-MFNP. For the fine examination of the targeting event on a microscopic scale, the cellular affinity of G-MFNP was investigated using dark-field microscopy. Dark-field microscopy is a simple, effective, and low-cost technique for confirming the interaction between nanoparticles and cells [37]. While a dark background around cells was seen in both HepG2 and MCF7 cells without G-MFNP, HepG2 cells showed numerous vivid and bright white dots, preferentially outside the cells, by scattering the

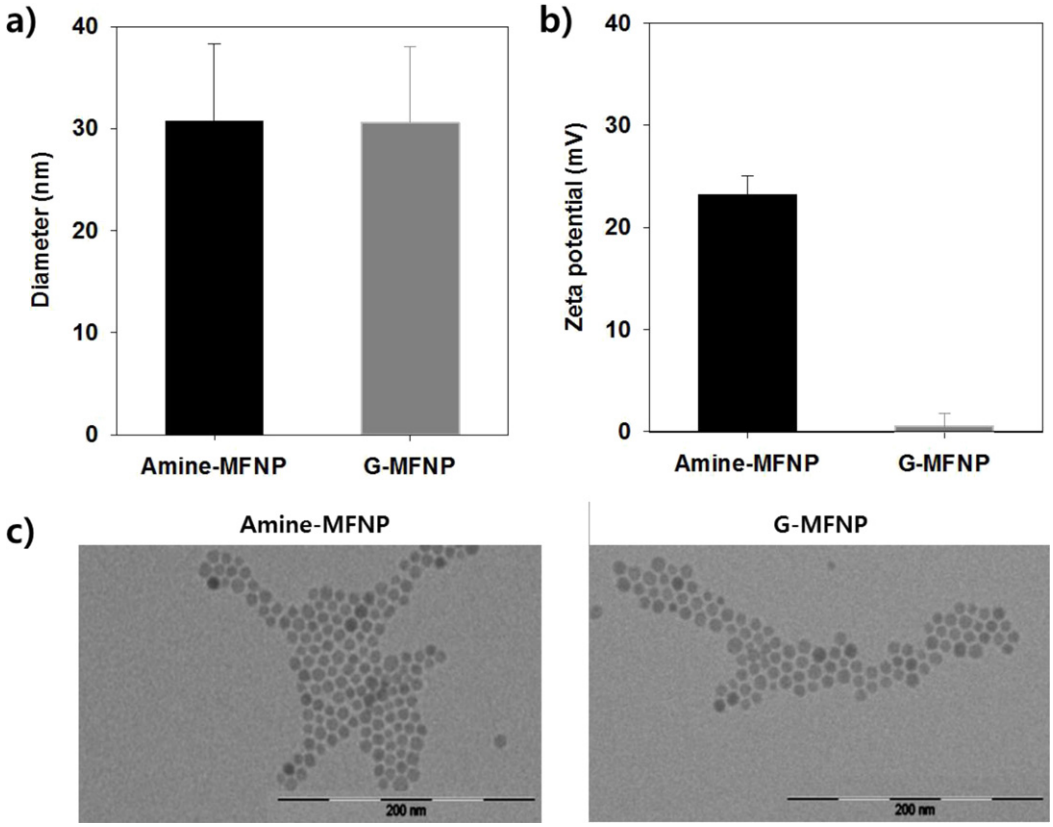

Figure 3. (a) Colloidal size distribution, (b) zeta potential of amine-MFNP and G-MFNP. (c) TEM images of amine-MFNP (left) and G-MFNP (right).

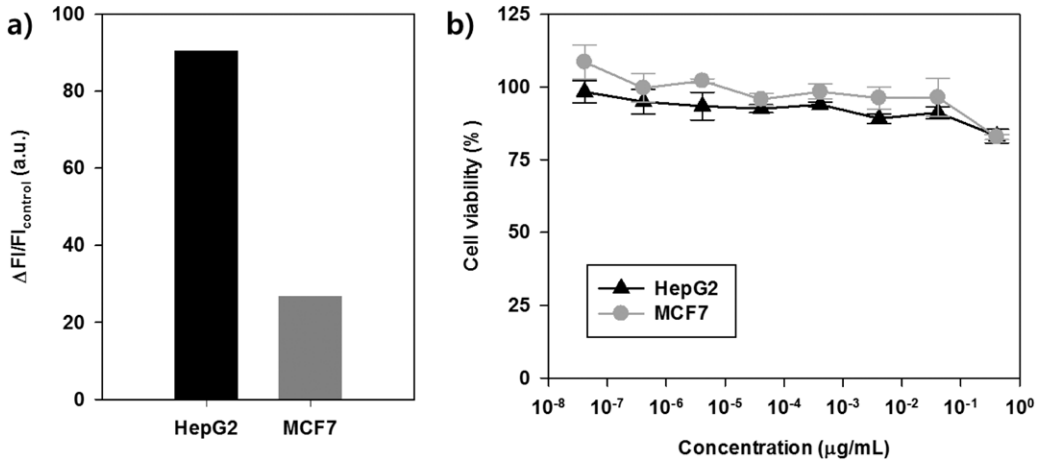

Figure 4. (a) Relative fluorescent intensity (FI: fluorescence intensity, control: non-treatment cells) of HepG2 and MCF7 cell lines using 1 mM fluorescein amine-gal conjugates via flow cytometry analysis for HepG2 and MCF7 cells treated with galactosyl fluorescein via flow cytometry analysis. (b) Cell viabilities for HepG2 and MCF7 cells after treatment with G-MFNP.

incident light by MFNP (figure 5(a)). MCF7 cells treated with G-MFNP exhibited no change in appearance of a bright spot compared to the cells without G-MFNP, this phenomenon indicates that G-MFNP specifically bind to the ASGPr of the HepG2 cell membranes. To evaluate the presence of magnetic components in G-MFNP-treated cells, Prussian blue staining was carried out. The magnetic ions, in cells treated with G-MFNP, were combined with injected ferrocyanide, resulting in the appearance of a bright blue color. In figure 5(b), the specific cellular affinity of G-MFNP for HepG2 cells was also observed by the blue spots due to Prussian blue staining.

Receptor-mediated endocytosis is a common phenomenon for the uptake of molecules by cells and the ASGPr is one of the best-studied endocytotic transport receptors [38]. After binding of ligands to receptors, the receptor–ligand complex migrates along the plane of the plasma membrane to a site of active internalization. However,

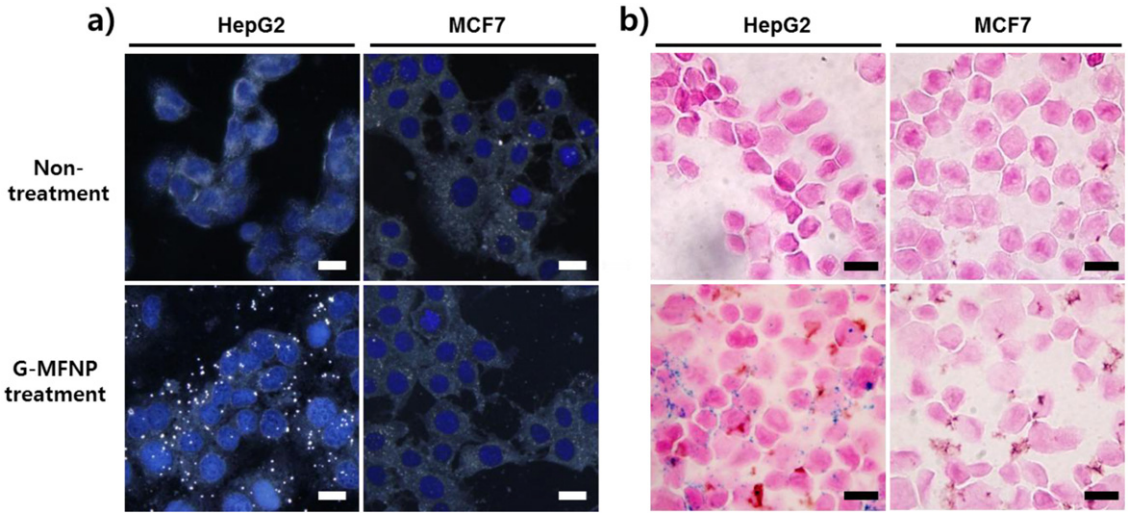

Figure 5. (a) Dark-field microscopy and (b) Prussian blue staining images of HepG2 and MCF7 cells treated with G-MFNP. The scale bar is 10 μm.

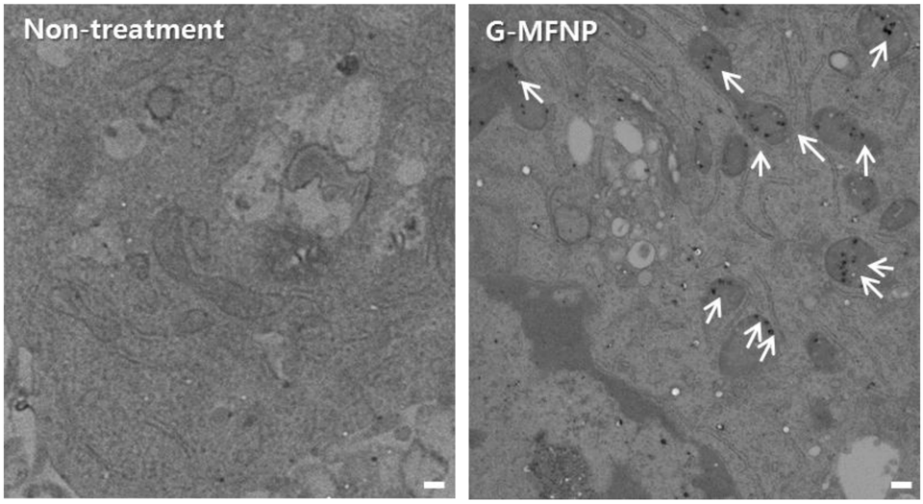

Figure 6. TEM images of untreated control HepG2 cells and G-MFNP-treated HepG2 cells (scale bar: 200 nm).

the above results do not prove whether G-MFNP exist in cytosol. To confirm whether binding of G-MFNP to the ASGPr results in subsequent receptor-mediated endocytosis, G-MFNP-treated HepG2 cells were observed by transmission electron microscopy. The cellular morphology after treatment with nanoparticles did not result in obvious changes. The nuclear membranes of the treated cells were intact, and no apoptotic bodies were visible in the cells. Galactosyl MFNP was observed in the endosomal confines of cytoplasm as aggregated forms (figure 6, arrows). We also carried out quantitative analysis of the targeting efficiency of G-MFNP for ASGPr using absorbance spectra analysis. This analysis method can quantitate the amount of attached G-MFNP toward HepG2 and MCF7 because the magnetic nanoparticles have a characteristic absorbance band around 410 nm. After treating G-MFNP to cells, there was little change in absorbance for either HepG2 or MCF7 up to 1 h. After 2 h, however, the absorbance of HepG2 is observed to increase by approximately 160% relative to MCF7 (figure 7(b)). After incubation for 8 h, the cellular affinity of G-MFNP for MCF7 cells increased slightly, probably due to non-specific binding (data not shown). These results demonstrate that G-MFNP have a very specific binding property for ASGPr.

The targeting potential of G-MFNP for ASGPr was investigated by MRI. In $T2$-weighted MR images, HepG2 cells were identified in black after treatment with G-MFNP, while MCF7 cells treated with G-MFNP appeared gray (figure 8(a)). The MR signal intensity ($\Delta R2/R2_{\text{control}}$) for HepG2 cells treated with G-MFNP was higher than that of MCF7 cells treated with G-MFNP by a factor of 2.2 (figure 8(b)). We also conducted a quantitative analysis of HepG2 cells treated with G-MFNP using two kinds of spectroscopy. Firstly, the amount (magnetic ions: iron and manganese) of treated G-MFNP bound to cells was estimated using inductively coupled plasma atomic emission spectroscopy (figure 7(a)). HepG2 cells treated with G-MFNP showed a higher affinity than MCF7 cells treated with G-MFNP by a factor of 1.8.

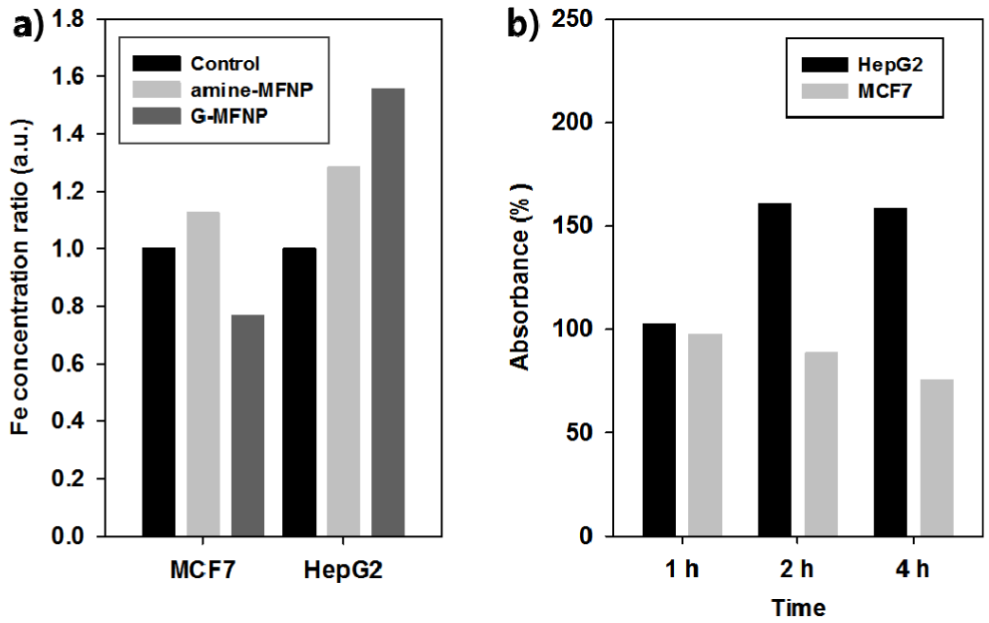

Figure 7. (a) Uptake efficacy for HepG2 and MCF7 cells treated with G-MFNP obtained by ICP-AES. (b) Absorbance ratio graph for HepG2 cells and MCF7 cells treated with G-MFNP in ($\lambda = 410$ nm, control: untreated cells).

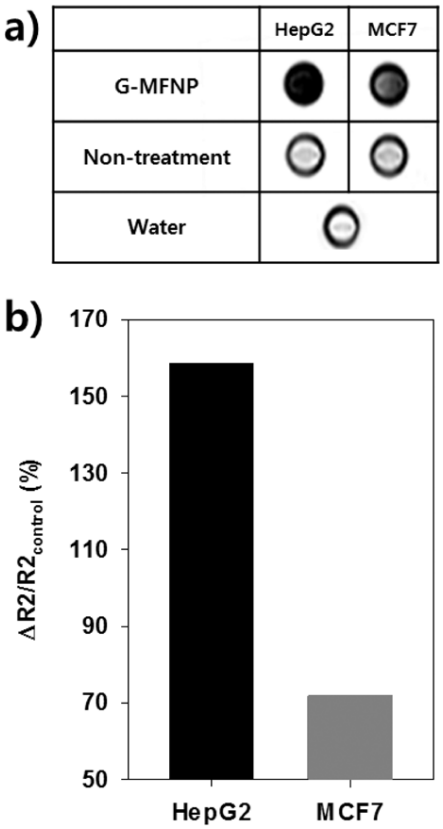

Figure 8. (a) MR images and (b) $\Delta R2/R2_{control}$ graph of HepG2 and MCF7 cells treated with G-MFNP.

4. Conclusions

We developed a *T*2 MR imaging nanoprobe allowing ASGPr-specific imaging. We synthesized MFNP conjugated with galactosylgluconic acid for the galactosylation of the surface of the nanoprobe. The interaction with and internalization of G-MFNP by ASGPr-expressing cancer cells were confirmed by various methodologies, such as absorbance, dark-field microscopy, Prussian blue staining, and cellular transmission electron microscopy. These results strongly suggest that G-MFNP have excellent selectivity toward ASGPr-expressing cancer cells. In addition, G-MFNP enable MR imaging of ASGPr, reflecting that G-MFNP will be helpful in the diagnosis and treatment of liver disease because the level of ASGPr expression is closely associated with acute hepatitis, chronic hepatitis, autoimmune hepatitis, cirrhosis [9–11], liver cancers [21] and also cancer metastasis [12]. In future studies, the evaluation of G-MFNP as a contrast agent for real-time monitoring of tumor progression will be required using a xenograft animal model.

Acknowledgment

This work was supported by the National Research Foundation of Korea (NRF) grant funded by the Korea Government (MEST) (2011-0027623) and a grant from the National R&D Program for Cancer Control, Ministry for Health and Welfare, Republic of Korea (1020390).

References

[1] McCann T E, Kosaka N, Turkbey B, Mitsunaga M, Choyke P L and Kobayashi H 2011 Molecular imaging of tumor invasion and metastases: the role of MRI *NMR Biomed.* **24** 561–8

[2] Skotland T 2012 Molecular imaging: challenges of bringing imaging of intracellular targets into common clinical use *Contrast Media Mol. I.* **7** 1–6

[3] Weissleder R and Pittet M J 2008 Imaging in the era of molecular oncology *Nature* **452** 580–9

[4] Lee J-H *et al* 2007 Artificially engineered magnetic nanoparticles for ultra-sensitive molecular imaging *Nature Med.* **13** 95–9

[5] Cho E J, Yang J, Mohamedali K A, Lim E K, Kim E J, Farhangfar C J, Suh J S, Haam S, Rosenblum M G and Huh Y M 2011 Sensitive angiogenesis imaging of orthotopic bladder tumors in mice using a selective magnetic resonance imaging contrast agent containing VEGF 121/rGel *Invest. Radiol.* **46** 441–9

[6] Yang J *et al* 2007 Synthesis of ultrasensitive magnetic resonance contrast agents for cancer imaging using PEG-fatty acid *Chem. Mater.* **19** 3870–6

[7] Ashwell G and Harford J 1982 Carbohydrate-specific receptors of the liver *Annu. Rev. Biochem.* **51** 531–54

[8] Weigel P H and Oka J A 1983 The large intracellular pool of asialoglycoprotein receptors functions during the endocytosis of asialoglycoproteins by isolated rat hepatocytes *J. Biol. Chem.* **258** 5095–102

[9] Dalekos G N, Zachou K, Liaskos C and Gatselis N 2002 Autoantibodies and defined target autoantigens in autoimmune hepatitis: an overview *Eur. J. Intern. Med.* **13** 293–303

[10] Reimer P, Weissleder R, Lee A S, Buettner S, Wittenberg J and Brady T J 1991 Asialoglycoprotein receptor function in benign liver-disease: evaluation with MR imaging *Radiology* **178** 769–74

[11] Zachou K, Rigopoulou E and Dalekos G N 2004 Autoantibodies and autoantigens in autoimmune hepatitis: important tools in clinical practice and to study pathogenesis of the disease *J. Autoimmun.* **1** 2

[12] Ueno S, Mojic M, Ohashi Y, Higashi N, Hayakawa Y and Irimura T 2011 Asialoglycoprotein receptor promotes cancer metastasis by activating the EGFR-ERK pathway *Cancer Res.* **71** 6419–27

[13] Ciechanover A, Schwartz A L and Lodish H F 1983 Sorting and recycling of cell surface receptors and endocytosed ligands: the asialoglycoprotein and transferrin receptors *J. Cell. Biochem.* **23** 107–30

[14] Goto M, Yura H, Chang C W, Kobayashi A, Shinoda T, Maeda A, Kojima S, Kobayashi K and Akaike T 1994 Lactose-carrying polystyrene as a drug carrier—investigation of body distributions to parenchymal liver-cells using I-125 labeled lactose-carrying polystyrene *J. Control. Release* **28** 223–33

[15] Kato Y, Onishi H and Machida Y 2001 Biological characteristics of lactosaminated *N*-succinyl-chitosan as a liver-specific drug carrier in mice *J. Control. Release* **70** 295–307

[16] Nishikawa M, Kamijo A, Fujita T, Takakura Y, Sezaki H and Hashida M 1993 Synthesis and pharmacokinetics of a new liver-specific carrier, glycosylated carboxymethyl-dextran, and its application to drug targeting *Pharm. Res.* **10** 1253–61

[17] Arangoa M A, Duzgunes N and Tros de Ilarduya C 2003 Increased receptor-mediated gene delivery to the liver by protamine-enhanced-asialofetuin-lipoplexes *Gene Ther.* **10** 5–14

[18] Sliedregt L A J M, Rensen P C N, Rump E T, van Santbrink P J, Bijsterbosch M K, Valentijn A R P M, van der Marel G A, van Boom J H, van Berkel T J C and Biessen E A L 1999 Design and synthesis of novel amphiphilic dendritic galactosides for selective targeting of liposomes to the hepatic asialoglycoprotein receptor *J. Med. Chem.* **42** 609–18

[19] Joziasse D H, Lee R T, Lee Y C, Biessen E A L, Schiphorst W E C M, Koeleman C A M and van den Eijnden D H 2000 Alpha 3-galactosylated glycoproteins can bind to the hepaticasialoglycoprotein receptor *Eur. J. Biochem.* **267** 6501–8

[20] Kawakami S, Yamashita F, Nishikawa M, Takakura Y and Hashida M 1998 Asialoglycoprotein receptor-mediated gene transfer using novel galactosylated cationic liposomes *Biochem. Biophys. Res. Commun.* **252** 78–83

[21] Reimer P, Weissleder R, Lee A S, Wittenberg J and Brady T J 1990 Receptor imaging: application to MR imaging of liver-cancer *Radiology* **177** 729–34

[22] Yang W, Pan C Y, Liu X Q and Wang J 2011 Multiple functional hyperbranched poly(amido amine) nanoparticles: synthesis and application in cell imaging *Biomacromolecules* **12** 1523–31

[23] Shen Z, Wei W, Tanaka H, Kohama K, Ma G, Dobashi T, Maki Y, Wang H, Bi J and Dai S 2011 A galactosamine-mediated drug delivery carrier for targeted liver cancer therapy *Pharmacol. Res.* **64** 410–9

[24] Kikkeri R, Lepenies B, Adibekian A, Laurino P and Seeberger P H 2009 *In vitro* imaging and *in vivo* liver targeting with carbohydrate capped quantum dots *J. Am. Chem. Soc.* **131** 2110–2

[25] Medina S H, Tekumalla V, Chevliakov M V, Shewach D S, Ensminger W D and El-Sayed M E H 2011 *N*-acetylgalactosamine-functionalized dendrimers as hepatic cancer cell-targeted carriers *Biomaterials* **32** 4118–29

[26] Huang G, Diakur J, Xu Z and Wiebe L I 2008 Asialoglycoprotein receptor-targeted superparamagnetic iron oxide nanoparticles *Int. J. Pharm.* **360** 197–203

[27] Luo Z, Cai K, Hu Y, Zhao L, Liu P, Duan L and Yang W 2011 Mesoporous silica nanoparticles end-capped with collagen: redox-responsive nanoreservoirs for targeted drug delivery *Angew. Chem. Int. Edn* **50** 640–3

[28] Akinc A *et al* 2010 Targeted delivery of RNAi therapeutics with endogenous and exogenous ligand-based mechanisms *Mol. Ther.* **18** 1357–64

[29] Hosseinkhani H, Aoyama T, Ogawa O and Tabata Y 2002 Liver targeting of plasmid DNA by pullulan conjugation based on metal coordination *J. Control. Release* **83** 287–302

[30] Lim E K, Yang J, Suh J S, Huh Y M and Haam S 2009 Self-labeled magneto nanoprobes using tri-aminated polysorbate 80 for detection of human mesenchymal stem cells *J. Mater. Chem.* **19** 8958–63

[31] Hermanson G T 2008 *Bioconjugate Techniques* 2nd edn (Amsterdam: Elsevier) pp 219–23

[32] Seo S-B, Yang J, Hyung W, Cho E-J, Lee T-I, Song Y J, Yoon H-G, Suh J-S, Huh Y-M and Haam S 2007 Novel multifunctional PHDCA/PEI nano-drug carriers for simultaneous magnetically targeted cancer therapy and diagnosis via magnetic resonance imaging *Nanotechnology* **18** 475105

[33] Yang S-H, Heo D, Park J, Na S, Suh J-S, Haam S, Park S W, Huh Y-M and Yang J 2012 Role of surface charged manganese ferrite nanoparticles towards macrophages *Nanotechnology* **23** 505702

[34] Lu J, Zhu D, Zhang Z R, Hai L, Wu Y and Sun X 2010 Novel synthetic LPDs consisting of different cholesterol derivatives for gene transfer into hepatocytes *J. Drug Target.* **18** 520–35

[35] Duan C, Gao J, Zhang D, Jia L, Liu Y, Zheng D, Liu G, Tian X, Wang F and Zhang Q 2011 Galactose-decorated pH-responsive nanogels for hepatoma-targeted delivery of oridonin *Biomacromolecules* **12** 4335–43

[36] Jain V, Nath B, Gupta G K, Shah P P, Siddiqui M A, Pant A B and Mishra P R 2009 Galactose-grafted chylomicron-mimicking emulsion: evaluation of specificity against HepG-2 and MCF-7 cell lines *J. Pharm. Pharmacol.* **61** 303–10

[37] Choi R, Yang J, Choi J, Lim E K, Kim E, Suh J S, Huh Y M and Haam S 2010 Thiolated dextran-coated gold nanorods for photothermal ablation of inflammatory macrophages *Langmuir* **26** 17520–7

[38] Spiess M 1990 The asialoglycoprotein receptor: a model for endocytic transport receptors *Biochemistry* **29** 10009–18